On the Numerical Stability of Simulation Methods for SDEs

Eckhard Platen[1] and **Lei Shi**[2]

November 7, 2009

Abstract. When simulating discrete time approximations of solutions of stochastic differential equations (SDEs), in particular martingales, numerical stability is clearly more important than some higher order of convergence. Discrete time approximations of solutions of SDEs are widely used in simulation in finance. The stability criterion presented in this paper is designed to handle both scenario and Monte Carlo simulation, that is, both strong and weak approximations. Methods are identified that have the potential to overcome some of the numerical instabilities experienced when using the explicit Euler scheme. This is of particular importance in finance, where frequently martingale dynamics arise and diffusion coefficients are often multiplicative. Stability regions for various schemes are visualized and analyzed. The result being that schemes, which have implicitness in both the drift and the diffusion terms, exhibit the largest stability regions. Most importantly it will be shown that by refining the time step size, one can leave a stability region and may incur numerical instabilities, which is not what one typically experiences in deterministic numerical analysis.

1991 *Mathematics Subject Classification:* primary 65C20; secondary 60H10.
Key words and phrases: Stochastic differential equations, scenario simulation, Monte Carlo simulation, numerical stability, predictor-corrector methods, implicit methods.

[1]University of Technology, Sydney, School of Finance & Economics and Department of Mathematical Sciences, PO Box 123, Broadway, NSW, 2007, Australia
[2]University of Technology, Sydney, Australia, School of Finance & Economics

1 Introduction

Simulation methods for the approximate solution of stochastic differential equations (SDEs) are some of the most widely used quantitative tools in finance. Monographs describing these methods include, for instance, Kloeden & Platen (1999), Milstein (1995), Kloeden, Platen & Schurz (2003), Jäckel (2002), Higham (2004) and Glasserman (2004). Not everyone who uses these schemes in scenario or Monte Carlo simulation is completely aware of the potential numerical stability problems that can make a simulation meaningless. If the propagation of the naturally arising errors in a scenario simulation remains uncontrolled, then the simulated path may diverge substantially from the exact solution. Similarly, the estimate of a functional simulated via the Monte Carlo method, may significantly differ from the exact expectation of the functional due to numerical stability issues. It is well known for larger time step sizes that explicit methods, in particular the widely used Euler method, work unreliably and may generate large errors. This has been pointed out, for instance by Milstein, Platen & Schurz (1998) for the case of driftless SDEs with multiplicative noise. For illustration, consider the driftless Black-Scholes SDE

$$dX_t = X_t b \, dW_t \tag{1.1}$$

for $t \geq 0$ and $X_0 = 1$, as it typically appears in the simulation of discounted asset prices under the risk-neutral measure. The asset price process $X = \{X_t, t \geq 0\}$ is in this example chosen to be a martingale, with b denoting the volatility. Here $W = \{W_t, t \geq 0\}$ represents a standard Wiener process under the pricing measure $\mathbb{P}$. In Figure 1.1 we exhibit an exact path of the geometric Brownian motion given in (1.1) for $b = 1$, and show also a discrete time approximation obtained by the Euler scheme

$$Y_{n+1} = Y_n + Y_n \;\; b\Delta W_n \tag{1.2}$$

for $t_n = n\Delta$ with $\Delta = 2$ and $\Delta W_n = W_{t_n+\Delta} - W_{t_n}$. One notes that a significant error is building up over time. It will become clear later that this is the result of a numerical instability.

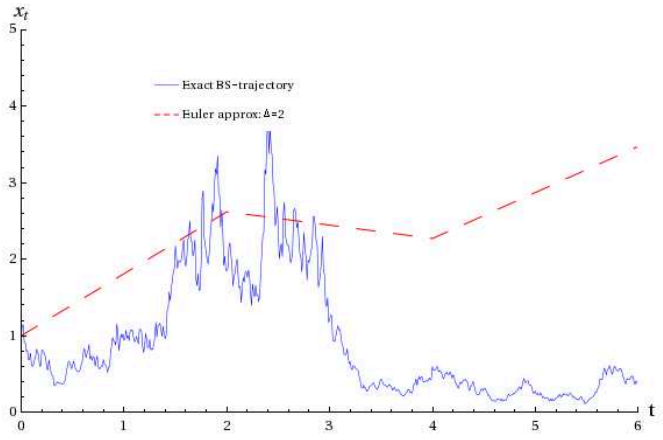

Figure 1.1: Exact BS-trajectory and Euler approximation..

In another example we use a simplified Euler scheme with independent, two-point distributed random variables representing ΔW_n in (1.2), such that $P(\Delta W_n = \pm\sqrt{\Delta}) = 1/2$. We approximate via Monte Carlo simulation the first absolute moment $E(|X_T|)$ for $T \in [0, 20]$, and show in Figure 1.2, for the case $b = 1$ and $\Delta = 2$ the absolute error obtained when using 100,000 sample paths. This example reveals that the error becomes significant. Also in this case we will see that this behavior is caused by numerical instability.

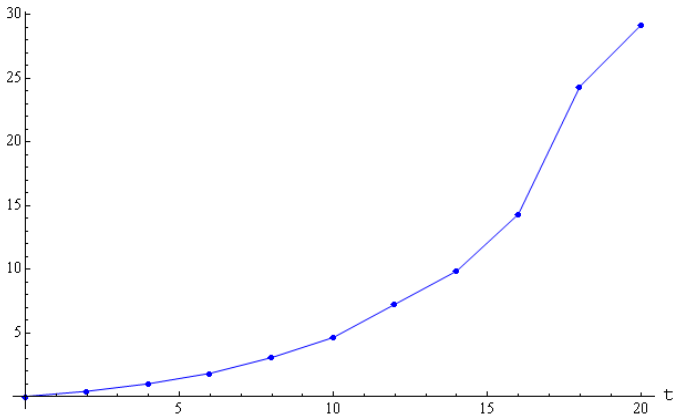

Figure 1.2: Absolute error of the simulated first absolute moment for the simplified Euler scheme.

Implicit and predictor-corrector methods can be successfully used to control the propagation of errors, see for instance, Talay (1982), Klauder & Petersen (1985), Milstein (1988), Hernandez & Spigler (1992, 1993), Saito & Mitsui (1993a, 1993b), Kloeden & Platen (1992, 1999), Milstein, Platen & Schurz (1998), Higham (2000), Alcock & Burrage (2006) and Higham, Mao & Yuan (2007). For strong approximate solutions of SDEs, it is non trivial to introduce implicitness into the discrete time approximation of the diffusion terms. For SDEs with zero drift, as is often encountered in finance when modeling martingales, there is no possibility for generating implicitness in the drift term in a scheme. Balanced implicit methods may help to stabilize the numerical approximation in such a situation, see Milstein, Platen & Schurz (1998) and Alcock & Burrage (2006). Predictor-corrector methods, proposed in Platen (1995) and Bruti-Liberati & Platen (2008), can also improve the numerical stability.

The aim of the current paper is to provide some insights into the numerical stability of schemes for the discrete time approximation of SDEs. We introduce a numerical stability criterion that allows one to visualize corresponding stability regions. Several numerical stability concepts proposed in the literature can be conveniently linked to the suggested criterion. The numerical stability of a method is examined using a family of linear test equations with multiplicative noise. The visualization of the resulting stability regions for different schemes is an important aspect of our study. This allows one to make informed decisions when selecting a scheme for a given scenario or Monte Carlo simulation in finance or to explain and predict numerical failures. An interesting observation is that for

some SDEs and schemes a refinement of the time discretization can lead to numerical instabilities, which is inconsistent with what one expects in deterministic numerical analysis.

This paper is organized as follows: Section 2 introduces a concept of numerical stability. In Section 3, stability regions for various predictor-corrector methods are discussed. Section 4 studies the stability regions of particular implicit schemes. Finally, Section 5 discusses the numerical stability of a range of methods that are designed for Monte Carlo simulation.

2 Asymptotic p-Stability

In conjunction with the widely discussed concepts of strong or weak order convergence, the question of numerical stability should be answered when deciding on which numerical scheme to use. Various concepts of numerical stability have been introduced in the literature. These concepts typically make use of specifically designed test equations, which have explicit solutions available, see for instance, Milstein (1995), Kloeden & Platen (1999), Hernandez & Spigler (1992, 1993), Saito & Mitsui (1993a, 1993b, 1996), Hofmann & Platen (1994, 1996), Higham (2000) and Higham, Mao & Yuan (2007).

Stability regions have been identified for the parameter sets where the propagation of errors is under control in a well-defined sense. In some cases authors use solutions of complex valued linear SDEs with additive noise as test dynamics, see Milstein (1995), Kloeden & Platen (1999) and Hernandez & Spigler (1992, 1993) and Higham (2000). In financial applications, these test equations may potentially not be realistic enough to capture numerical instabilities that could arise when simulating asset prices. Typical martingale SDEs have no drift, and their diffusion coefficients are often level dependent in an approximately multiplicative manner. To study the error propagation of corresponding numerical schemes, test SDEs with multiplicative noise have been suggested in real and complex valued form, see Saito & Mitsui (1993a, 1993b, 1996), Hofmann & Platen (1994, 1996), Higham (2000) and Bruti-Liberati & Platen (2008).

The current paper introduces a relatively general stability criterion. It unifies in some sense criteria that measure so called: asymptotic stability, mean square stability, p-stability and the stability of absolute moments. A corresponding stability region can be visualized, allowing us to study the stability properties for a variety of both strong and weak numerical schemes.

Similar to Hofmann & Platen (1994) and Bruti-Liberati & Platen (2008) we use a *linear test SDE* with *multiplicative noise*

$$dX_t = \left(1 - \frac{3}{2}\,\alpha\right) \lambda\, X_t\, dt + \sqrt{\alpha\,|\lambda|}\, X_t\, dW_t \tag{2.1}$$

for $t \geq 0$, where $X_0 > 0$, $\lambda < 0$, $\alpha \in [0, 1)$. Here we call α the degree of stochasticity and λ the growth parameter. The corresponding Stratonovich SDE has the form

$$dX_t = (1 - \alpha)\,\lambda\, X_t\, dt + \sqrt{\alpha\,|\lambda|}\, X_t \circ dW_t, \tag{2.2}$$

where "$\circ$" denotes the Stratonovich stochastic integral, see Kloeden & Platen (1999).

For the two equivalent real valued SDEs (2.1) and (2.2), the parameter $\alpha \in [0, 1)$ describes the degree of stochasticity of the test dynamics. When $\alpha = 0$, the SDEs (2.1) and (2.2) become deterministic.

In the case $\alpha = \frac{2}{3}$, the Itô SDE (2.1) has no drift, and X is a martingale. This case models typical asset price dynamics when the price is expressed in units of the numéraire under the corresponding pricing measure. When the numéraire is the savings account, then the pricing measure is, under appropriate assumptions, the risk neutral probability measure. Platen & Heath (2006) show that the pricing measure is the real-world probability measure when the numéraire is taken to be the numéraire portfolio. In the case $\alpha = 1$, the Stratonovich SDE (2.2) has no drift. This is also the largest α for which the dynamics in (2.1) are potentially useful test dynamics, when focusing on negative growth parameters $\lambda < 0$.

We will rely on the following notion of stability, see also Hasminski (1980):

Definition 2.1 *For $p > 0$ a process $Y = \{Y_t, t > 0\}$ is called asymptotically* p-stable *if*

$$\lim_{t \to \infty} E(|Y_t|^p) = 0. \tag{2.3}$$

Consequently, a process is asymptotically p-stable if in the long run its pth moment vanishes. By the Lyapunov inequality it follows that if a process is asymptotically p_1-stable, for $p_1 > p_2 > 0$, then it is also asymptotically p_2 stable. The explicit solution of (2.1) and (2.2) is of the form

$$X_t = X_0\, \exp\left\{(1 - \alpha)\,\lambda\, t + \sqrt{\alpha\,|\lambda|}\, W_t\right\} \tag{2.4}$$

for $t \geq 0$, $\lambda < 0$ and $\alpha \geq 0$. For $p > 0$ and $\lambda < 0$ it follows from (2.4), by application of Itô's formula and taking expectation, that

$$\lim_{t \to \infty} E(|X_t|^p) = 0 \tag{2.5}$$

if and only if $\alpha < \frac{1}{1+\frac{p}{2}}$. This means that in the case when $\lambda < 0$ and $\alpha \in [0, \frac{1}{1+p/2})$, X is asymptotically p-stable. Furthermore, note for $\lambda < 0$ that by the law of iterated logarithm and the law of large numbers, one has

$$P\left(\lim_{t \to \infty} X_t = 0\right) = 1 \tag{2.6}$$

if and only if $\alpha \in [0, 1)$, see for instance Protter (2005).

Since there is limited potential for identifying numerically stable schemes for unstable test dynamics, we will consider test dynamics given by (2.1) only for negative growth parameter $\lambda < 0$. Furthermore, as indicated previously, for $\lambda < 0$ it makes sense to restrict the degree of stochasticity to the range $\alpha \in [0, 1)$. With this parameter range we will also be able to detect schemes that are numerically stable for unstable test dynamics when α is above the border line $1/(1 + p/2)$ for given $p > 0$.

For simulation purposes, one would like to see a discrete time approximation Y and the original process X having similar stability properties. Ideally, for given $p > 0$ the approximation Y should generate asymptotically p-stable paths when X was asymptotically p-stable. In our subsequent analysis we will see that Y and X can have rather different stability properties for different combinations of values $\lambda\Delta$, α and p. To explore these differences, we introduce for a given discrete time approximation the notion of a *stability region*, which permits the convenient visualization of its asymptotic p-stability properties as a function of $\lambda\Delta, \alpha$ and p.

Definition 2.2 *The* stability region Γ *is determined by those triplets* $(\lambda\Delta, \alpha, p) \in (-\infty, 0) \times [0, 1) \times (0, \infty)$ *for which the discrete time approximation* Y *with time step size* Δ*, when applied to the test equation* (2.1)*, is asymptotically* p*-stable.*

In Monte Carlo simulation, where expectations of functionals are approximated, some moments of a discrete time approximation typically need to exhibit certain stability properties. Otherwise, errors in the expectations of functionals may be strongly propagated. To approximate well the finite pth moment of a stochastic process X, the numerical approximation Y needs to be asymptotically p-stable.

Note that the asymptotic p-stability criterion (2.3) can be related to other concepts of numerical stability introduced in the literature, such as the popular concept of mean-square stability, see Saito & Mitsui (1996), Higham (2000), Higham & Kloeden (2005) and Alcock & Burrage (2006). This particular concept, for some schemes leads to explicit characterizations of the resulting region of mean-square stability. However in general, stability regions need to be calculated numerically. The choice $p = 2$ is only a special one. Important information is gained by studying the change in the shape of the stability region as a function of p. When p increases, the cross section of the stability region of a numerical scheme shrinks as should be expected due to the Lyapunov inequality. We will see that typically it requires an implicit scheme to obtain, for instance for $p = 2$, a stability region that reaches beyond $\alpha = 0.5$. For comparison, recall that for $\lambda < 0$ and given $p \in (0, \infty)$ the test dynamics X are p-stable when $\alpha < \frac{1}{1+\frac{p}{2}}$.

We study in this paper the asymptotic p-stability for both strong and weak discrete time approximations of the test dynamics (2.2), where we focus on the parameter range $\lambda\Delta < 0$, $\alpha \in [0, 1)$ and $p \in (0, 2]$. This will provide for a p close

to 0 the widest stability region, which will turn out to be close to the stability region that refers to the type of asymptotic stability discussed in Bruti-Liberati & Platen (2008). For a given SDE with some form of multiplicative noise the following analysis provides some guidance to the choice of a particular scheme and time step size.

For many discrete time approximations Y with time step size $\Delta > 0$, when applied to the test equation (2.1) with a given degree of stochasticity $\alpha \in [0, 1)$, we observe that the ratio

$$\left| \frac{Y_{n+1}}{Y_n} \right| = G_{n+1}(\lambda \Delta, \alpha) \tag{2.7}$$

is of crucial interest, $n \in \{0, 1, \ldots\}$, $Y_n > 0$, $\lambda < 0$. We call the random variable $G_{n+1}(\lambda \Delta, \alpha)$ the *transfer function* of the approximation Y at time t_n. It transfers the previous approximate value Y_n to the approximate value Y_{n+1} of the next time step.

Furthermore, let us assume for a given scheme and given $\lambda < 0$, $\Delta \in (0, \infty)$ and $\alpha \in [0, 1)$ that the random variables $G_{n+1}(\lambda \Delta, \alpha)$ are for $n \in \{0, 1, \ldots\}$ independent and identically distributed with $E((\ln(G_{n+1}(\lambda \Delta, \alpha)))^2) < \infty$. This assumption is satisfied for a wide range of schemes, and will allow us to obtain the corresponding stability regions by employing the following result:

Lemma 2.3 *A discrete time approximation for a given $\lambda \Delta < 0$, $\alpha \in [0, 1)$ and $p > 0$, is asymptotically p-stable if and only if*

$$E((G_{n+1}(\lambda \Delta, \alpha))^p) < 1. \tag{2.8}$$

The proof of Lemma 2.3 is straightforward, since it is obvious from (2.7) that the pth moment of the approximation vanishes as $n \to \infty$, if and only if $E((G_{n+1}(\lambda \Delta, \alpha))^p) < 1$, for all $n \in \{0, 1, \ldots\}$.

Note for $p > 0$ that the condition (2.8) yields by the use of the inequality $\ln(x) \leq x - 1$, the relation

$$E(\ln(G_{n+1}(\lambda \Delta, \alpha))) \leq \frac{1}{p} E((G_{n+1}(\lambda \Delta, \alpha))^p - 1) < 0 \tag{2.9}$$

for all $n \in \{0, 1, \ldots\}$. When p vanishes this relation provides the previously indicated link to the criterion of asymptotic stability studied in Bruti-Liberati & Platen (2008). Note that a scheme is considered asymptotically stable for a given $\lambda\Delta$ and α if $E(\ln(G_{n+1}(\lambda \Delta, \alpha))) < 0$ for all $n \in \{0, 1, \ldots\}$.

In the following we visualize the stability regions of various schemes by identifying the set of triplets $(\lambda \Delta, \alpha, p)$ for which the inequality (2.8) is satisfied for $\lambda\Delta \in [-10, 0)$, $\alpha \in [0, 1)$ and $p \in (0, 2]$. We deliberately truncate the stability regions

at the level $p = 2$, since the area on the top provides information about the mean-square stability of the scheme. Of course, for higher values of p the stability region could also be visualized, the region will shrink further, and for some schemes it may become an empty set. Asymptotically, for very large p the stability region relates to the worst case stability concept studied in Hofmann & Platen (1994, 1996). As such, the employed asymptotic p-stability covers a relatively wide range of stability criteria with asymptotic stability on one end and worst case stability on the other end.

3 Stability of Predictor-Corrector Methods

Now, let us consider discrete time approximations for the solution $X = \{X_t, t \geq 0\}$ of the SDE

$$X_t = X_0 + \int_0^t a(X_s)\, ds + \int_0^t b(X_s)\, dW_s \tag{3.1}$$

for $t \geq 0$. The function $a : \Re \to \Re$ is the drift coefficient function. The function $b : \Re \to \Re$ denotes the diffusion coefficient function with respect to the Wiener process $W = \{W_t, t \geq 0\}$. Additionally, we use in our analysis below the adjusted drift function $\bar{a}_\eta$ for $\eta \in [0, 1]$ defined as

$$\bar{a}_\eta(x) = a(x) - \eta b(x) b'(x), \tag{3.2}$$

for $x \in \Re$, where $b'(x)$ denotes the first derivative of $b(.)$.

Consider a time discretization $0 = t_0 < t_1 < \ldots$ with equal time step size $\Delta = t_{n+1} - t_n$, $n \in \{0, 1, \ldots\}$. The corresponding increments of the Wiener process are denoted by $\Delta W_n = W_{t_{n+1}} - W_{t_n}$, $n \in \{0, 1, \ldots\}$. We denote by $Y_n = Y_{t_n}$ the value of a discrete time approximation at time t_n, and by $n_t = \max\{n \in \{0, 1, \ldots\} : t_n \leq t\}$ the largest integer n for which t_n does not exceed $t \geq 0$. The following strong predictor-corrector schemes generalize the Euler scheme, and can provide improved numerical stability. They avoid the need to solve an algebraic equation in each time step, as is required by implicit methods. At the nth time step, first the predictor is constructed by using an explicit Euler scheme which predicts a value $\bar{Y}_{n+1}$. The corrector is then applied, which is structurally similar to an implicit Euler scheme and corrects the predicted value. We emphasize that not only is the predictor step explicit, but also the corrector step, since it uses only the predicted value. We will see later that with such a predictor-corrector procedure one can attain stabilizing effects in the simulation. The *family of strong predictor-corrector Euler schemes* we consider, is given by the *corrector*

$$\begin{aligned} Y_{n+1} &= Y_n + \left\{\theta\, \bar{a}_\eta(\bar{Y}_{n+1}) + (1-\theta)\bar{a}_\eta(Y_n)\right\} \Delta \\ &\quad + \left\{\eta\, b(\bar{Y}_{n+1}) + (1-\eta)\, b(Y_n)\right\} \Delta W_n, \end{aligned} \tag{3.3}$$

and by the *predictor*

$$\bar{Y}_{n+1} = Y_n + a(Y_n)\, \Delta + b(Y_n)\, \Delta W_n. \tag{3.4}$$

Note that we need to employ in (3.3) the adjusted drift function $\bar{a}_\eta$ given in (3.2). We call the parameters $\theta, \eta \in [0,1]$ the degrees of implicitness of the drift and the diffusion coefficients, respectively. Obviously, for the case $\eta = \theta = 0$ one recovers the Euler scheme. A major advantage of the above family of schemes is that it offers flexible degrees of implicitness η and θ. For each possible combination of these two parameters the scheme is of strong order 0.5 in the sense of Kloeden & Platen (1999), see Bruti-Liberati & Platen (2008). This allows one to compare for a given problem simulated paths using different degrees of implicitness. If these paths differ significantly from each other, then some numerical stability problem is likely to be present and one needs to make an effort in providing more numerical stability. For the Euler scheme, which results for the choice $\theta = \eta = 0$

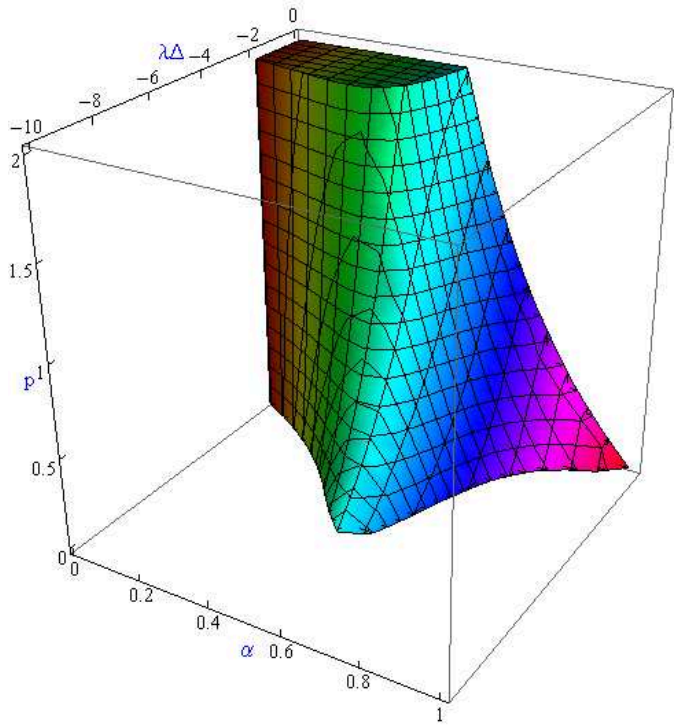

Figure 3.1: Stability region for the Euler scheme.

in (3.3), it follows by (2.7) that

$$G_{n+1}(\lambda\,\Delta, \alpha) = \left| 1 + \left(1 - \frac{3}{2}\,\alpha\right) \lambda\,\Delta + \sqrt{-\alpha\,\lambda}\,\Delta W_n \right|, \tag{3.5}$$

where $\Delta W_n \sim \mathcal{N}(0, \Delta)$ is a Gaussian distributed random variable with mean zero and variance Δ. The transfer function (3.5) yields the stability region that is shown in Figure 3.1. It is the region where $E((G_{n+1}(\lambda\,\Delta, \alpha))^p) < 1$. This stability region has been obtained numerically by identifying for each pair $(\lambda\Delta, \alpha) \in [-10, 0) \times [0, 1)$ those values $p \in (0, 2]$ for which the inequality (2.8) holds. One notes that for the purely deterministic dynamics of the test SDE, that is $\alpha = 0$, the stability region covers the area $(-2, 0) \times (0, 2)$. Also in later

figures we will observe that for $\alpha = 0$, we do not have any dependence on p. This is explained by the fact that in this case there is no stochasticity, and the relation $\lambda\Delta \in (-2, 0)$ reflects the classical interval of numerical stability for the Euler scheme, see Hairer & Wanner (1996). For a stochasticity parameter of about $\alpha \approx 0.5$, the stability region in Figure 3.1 has the largest cross section in the direction of $\lambda\,\Delta$ for most values of p. The stability region covers an interval for $\lambda\Delta$ of increasing length up to about $[-6.5, 0]$ when p is close to zero, and approximately $[-3, 0]$ when p increases to about 2. For increased stochasticity parameter α beyond 0.5 the stability region declines in Figure 3.1. We observe that if the Euler scheme is asymptotically p-stable for a certain step size, then it is also asymptotically p-stable for smaller step sizes. We see later that this is not always the case for other schemes.

The top of Figure 3.1 shows the mean-square stability region of the Euler scheme, where we have $p = 2$. As the order p of the moment increases, the cross section in the direction of α and $\lambda\Delta$ is reduced. The intuition is that as the stability requirements in terms of the order p of the moment becomes stronger, there are less pairs $(\lambda\Delta, \alpha)$ for which the simulated approximation's pth moment tends to zero.

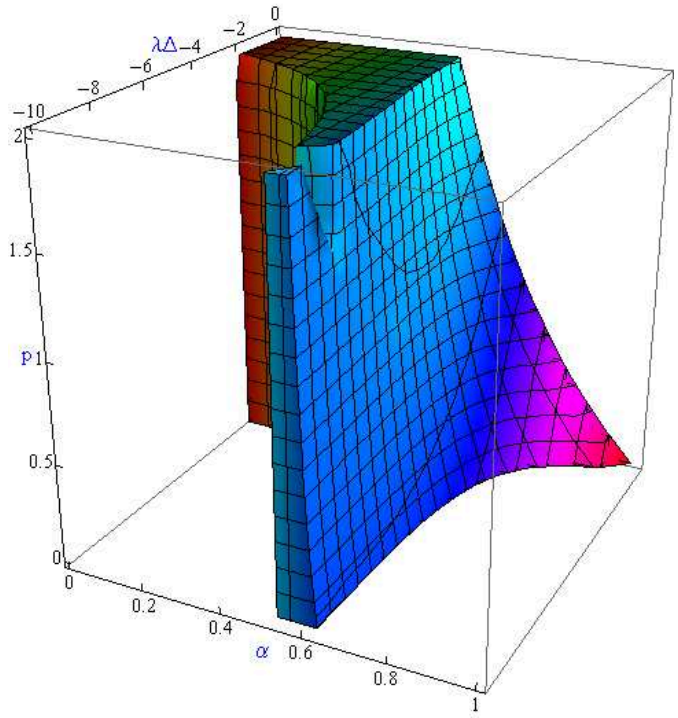

Figure 3.2: Stability region for semi-drift-implicit predictor-corrector Euler method.

Let us now consider the semi-drift-implicit predictor-corrector Euler method with

$\theta = \frac{1}{2}$ and $\eta = 0$ in (3.3). The transfer function for this method equals

$$G_{n+1}(\lambda\,\Delta, \alpha) \;=\; \left|1 + \lambda\,\Delta\left(1 - \frac{3}{2}\,\alpha\right)\left\{1 + \frac{1}{2}\left(\lambda\,\Delta\left(1 - \frac{3}{2}\,\alpha\right) + \sqrt{-\alpha\,\lambda}\,\Delta W_n\right)\right\} + \sqrt{-\alpha\,\lambda}\,\Delta W_n\right|.$$

Its stability region is displayed in Figure 3.2, showing that this scheme has good numerical stability around $\alpha \approx 0.6$, where it is stable for almost all $\lambda\Delta \in [-10, 0)$. When p is close to 2, its stability region begins to show a gouge around $\lambda\,\Delta \approx -9$. This means, when we consider the numerical stability of the second moment $p = 2$, instability could arise when using a step size close to $\lambda\Delta \approx -9$. Unfortunately, for the stochasticity parameter value $\alpha = \frac{2}{3}$, that is when X forms a martingale, the stability region is considerably reduced when compared to the region for $\alpha = 0.6$. Near the value of $\alpha = 0.6$ the semi-drift implicit predictor-corrector scheme outperforms the Euler scheme in terms of asymptotic p-stability for most values of p.

Similarly, we obtain for the drift-implicit predictor-corrector Euler method, derived from (3.3) with $\theta = 1$ and $\eta = 0$, the transfer function

$$G_{n+1}(\lambda\,\Delta, \alpha) \;=\; \left|1 + \lambda\,\Delta\left(1 - \frac{3}{2}\,\alpha\right)\left\{1 + \lambda\,\Delta\left(1 - \frac{3}{2}\,\alpha\right) + \sqrt{-\alpha\,\lambda}\,\Delta W_n\right\} + \sqrt{-\alpha\,\lambda}\,\Delta W_n\right|.$$

The corresponding stability region is plotted in Figure 3.3. It has similar features to the stability region of the semi-drift implicit predictor-corrector scheme. However, the stability region appears reduced. It no longer extends around $\alpha \approx 0.6$, as far in the negative direction of $\lambda\Delta$ as in Figure 3.2. When p is close to two, the gouge previously observed in Figure 3.2 near $\lambda\Delta \approx -9$, now occurs around $\lambda\Delta \approx -4$. It seems that the stability region decreased by making the drift fully "implicit". A balanced choice in (3.3) with $\theta = 1/2$ seems to be more appropriate than an extreme choice of full drift implicitness with $\theta = 1$.

Now, let us study the impact of making the diffusion term "implicit" in the predictor-corrector Euler method (3.3). First, we consider a predictor-corrector Euler method with semi-implicit diffusion term where $\theta = 0$ and $\eta = \frac{1}{2}$. Its transfer function has the form

$$G_{n+1}(\lambda\,\Delta, \alpha) \;=\; \left|1 + \lambda\,\Delta\,(1 - \alpha) + \sqrt{-\alpha\,\lambda}\,\Delta W_n \times \left\{1 + \frac{1}{2}\left(\lambda\,\Delta\left(1 - \frac{3}{2}\,\alpha\right) + \sqrt{-\alpha\,\lambda}\,\Delta W_n\right)\right\}\right|.$$

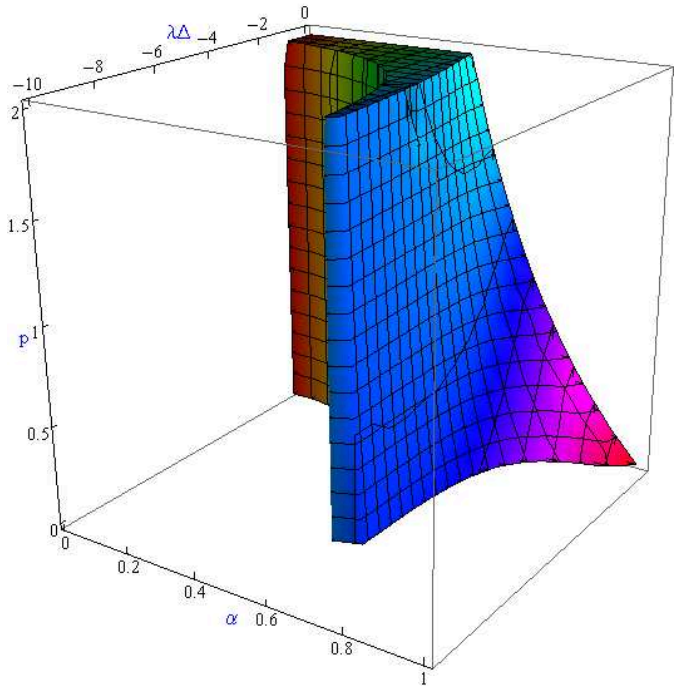

Figure 3.3: Stability region for drift-implicit predictor-corrector Euler method.

The corresponding stability region is shown in Figure 3.4. Although it seems to be rather restricted, when compared with the stability region for the semi-drift implicit predictor-corrector method, it is important to note that for the martingale case, that is $\alpha = \frac{2}{3}$, the stability region is here wider than those of the previous schemes. This observation could become relevant for simulations of martingales. Here one can only gain more numerical stability by making the diffusion term "implicit" rather than the drift term, as the latter is zero. Furthermore, although it may seem counter-intuitive, for this scheme one can actually lose numerical stability by reducing the time step size. For example, for small p near 0.01 and α near $\frac{2}{3}$, we observe that for about $\lambda\Delta \approx -3$ the method is asymptotically p-stable, whereas for smaller step sizes yielding a $\lambda\Delta$ above -2, the method is no longer asymptotically p-stable. Such a phenomenon is not common in deterministic numerical analysis. In stochastic numerics asymptotic p-stability may occasionally become lost for step sizes that are too small, as we will see also for some other schemes. In Figure 3.4 this phenomenon gradually disappears as the order of the moment p increases.

An interesting scheme is the symmetric predictor-corrector Euler method, ob-

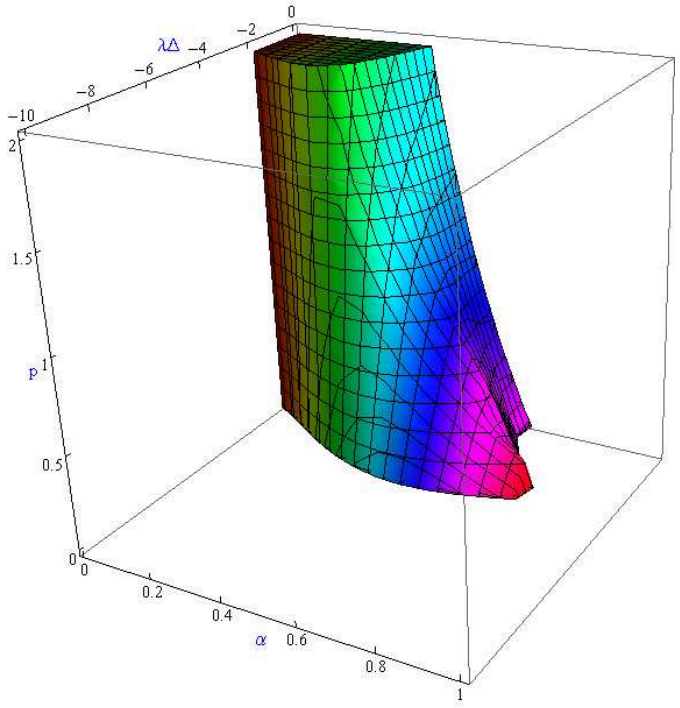

Figure 3.4: Stability region for the predictor-corrector Euler method with $\theta = 0$ and $\eta = \frac{1}{2}$.

tained from (3.3) for $\theta = \eta = \frac{1}{2}$. It has transfer function

$$G_{n+1}(\lambda\,\Delta, \alpha) \;=\; \left|1 + \lambda\,\Delta\,(1-\alpha)\left\{1 + \frac{1}{2}\left(\lambda\,\Delta\left(1 - \frac{3}{2}\,\alpha\right) + \sqrt{-\alpha\,\lambda}\,\Delta W_n\right)\right\}\right.$$
$$\left. + \sqrt{-\alpha\,\lambda}\,\Delta W_n\left\{1 + \frac{1}{2}\left(\lambda\,\Delta\left(1 - \frac{3}{2}\,\alpha\right) + \sqrt{-\alpha\,\lambda}\,\Delta W_n\right)\right\}\right|.$$

Its stability region is shown in Figure 3.5. In particular, for the martingale case $\alpha = \frac{2}{3}$ it has a rather large stability region when compared to that of the Euler scheme and those of previously discussed schemes. For p near zero, α close to one and $\lambda\,\Delta$ close to -1, there exists a small area where this scheme is not asymptotically p-stable. Again, this is an area where some decrease in the step size can make a simulation numerically unstable. As the value of p increases, this phenomenon disappears also here.

Next we check the stability region of a fully implicit predictor-corrector Euler method, which is obtained when setting in (3.3) both degrees of implicitness to

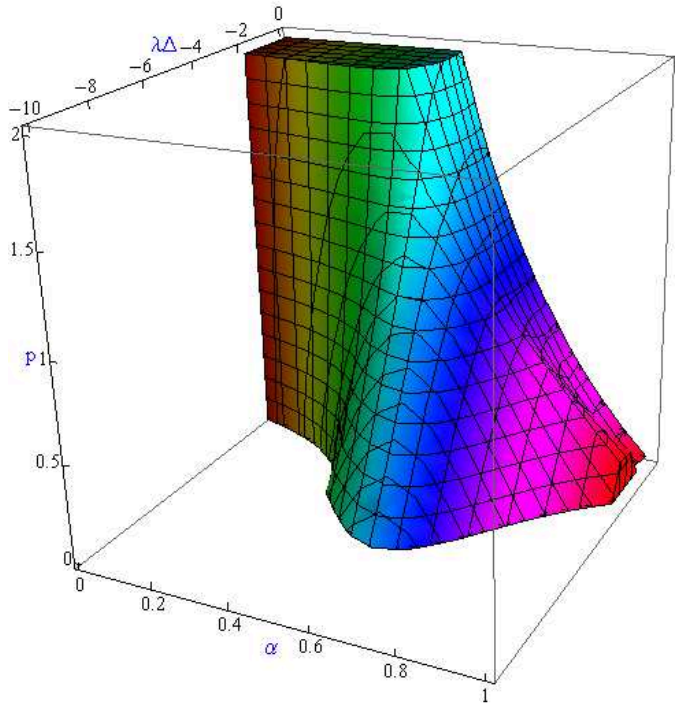

Figure 3.5: Stability region for the symmetric predictor-corrector Euler method.

one, that is $\theta = \eta = 1$. The corresponding transfer function is then of the form

$$\begin{aligned} G_{n+1}(\lambda\,\Delta, \alpha) \;&=\; \Big|1 + \lambda\,\Delta\left(1 - \frac{1}{2}\,\alpha\right)\left\{1 + \lambda\,\Delta\left(1 - \frac{3}{2}\,\alpha\right) + \sqrt{-\alpha\,\lambda}\,\Delta W_n\right\} \\ &\qquad + \sqrt{-\alpha\,\lambda}\,\Delta W_n\left\{1 + \lambda\,\Delta\left(1 - \frac{3}{2}\,\alpha\right) + \sqrt{-\alpha\,\lambda}\,\Delta W_n\right\}\Big| \\ &= \Big|1 + \left\{1 + \lambda\,\Delta\left(1 - \frac{3}{2}\,\alpha\right) + \sqrt{-\alpha\,\lambda}\,\Delta W_n\right\} \\ &\qquad \times \left\{\lambda\,\Delta\left(1 - \frac{1}{2}\,\alpha\right) + \sqrt{-\alpha\,\lambda}\,\Delta W_n\right\}\Big|\,. \end{aligned}$$

The resulting stability region is shown in Figure 3.6. We notice here that this stability region is considerably smaller than that of the symmetric predictor-corrector Euler scheme. It seems that the asymptotic p-stability does not increase monotonically with the degree of implicitness in both the drift and the diffusion term. Balanced levels of implicitness tend to achieve relatively large stability regions.

In summary, in the case of predictor-corrector Euler methods, the stability regions displayed suggest that the symmetric predictor-corrector Euler method, see Figure 3.5, is the most suitable of those visualized when simulating martingale dynamics under multiplicative noise. The symmetry between the drift and diffu-

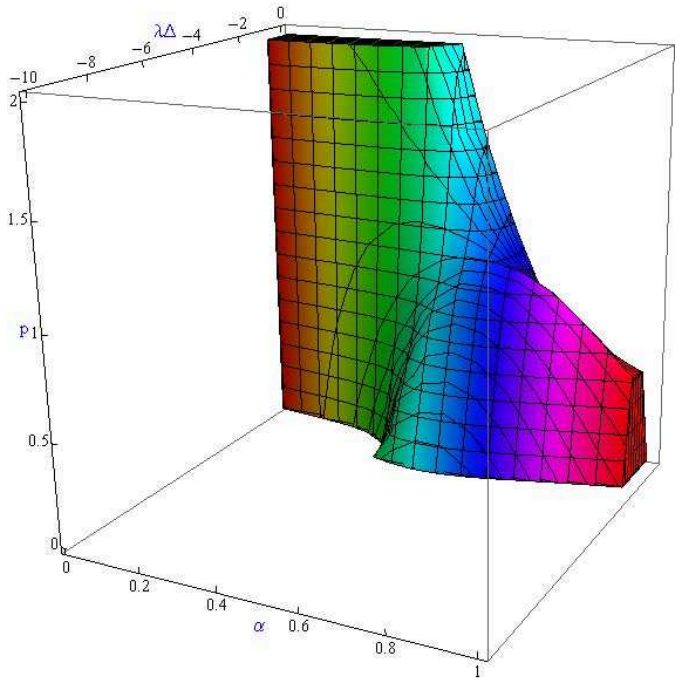

Figure 3.6: Stability region for fully implicit predictor-corrector Euler method.

sion terms of the method balances well its numerical stability properties, making it an appropriate choice for a range of simulation tasks.

4 Stability of Some Implicit Methods

After having studied the numerical stability properties of the family of predictor-corrector Euler methods (3.3), it is worthwhile to compare the observed stability regions with those of some implicit methods, which are known to show good numerical stability properties.

Let us first consider the semi-drift implicit Euler scheme in the form

$$Y_{n+1} = Y_n + \frac{1}{2}(a(Y_{n+1}) + a(Y_n))\Delta + b(Y_n)\Delta W_n.$$

It has the transfer function

$$G_{n+1}(\lambda\,\Delta, \alpha) = \left| \frac{1 + \frac{1}{2}\,\left(1 - \frac{3}{2}\,\alpha\right)\lambda\,\Delta + \sqrt{-\alpha\,\lambda}\,\Delta W_n}{1 - \frac{1}{2}\,\left(1 - \frac{3}{2}\,\alpha\right)\lambda\,\Delta} \right|. \tag{4.1}$$

Its stability region is shown in Figure 4.1. This kind of implicit scheme requires, in general, solving an algebraic equation at each time step in order to obtain

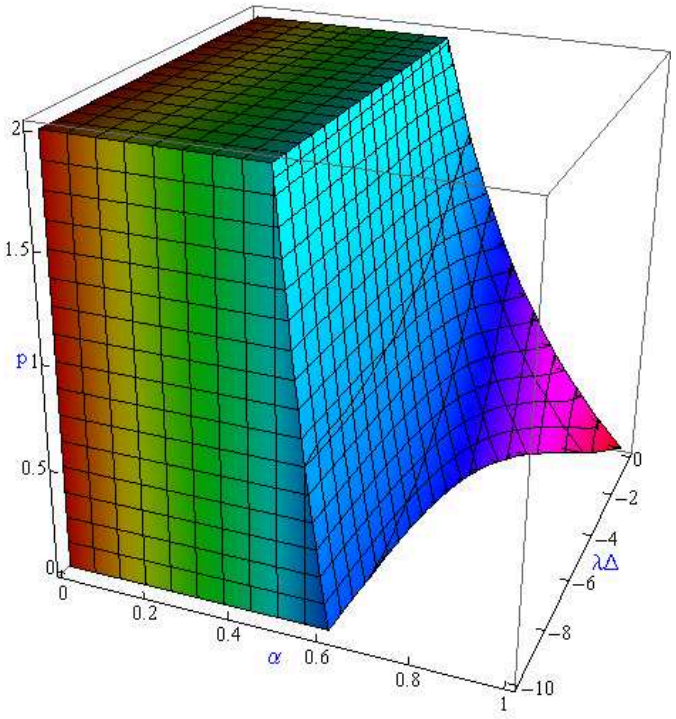

Figure 4.1: Stability region for semi-drift implicit Euler method.

the approximate solution. This extra computational effort makes the stability region significantly wider compared to those obtained for the previous predictor-corrector Euler schemes. For instance, for all considered values of p and $\lambda\,\Delta$, one obtains in Figure 4.1 always asymptotic p-stability for a degree of stochasticity of up to $\alpha = 0.5$. Unfortunately, there is no asymptotic p-stability for $\alpha = 2/3$ and for any values of p when $\lambda\,\Delta < -3$, which means that this numerical scheme may not be well suited for simulating martingale dynamics when the step size needs to remain large. The symmetric predictor-corrector Euler method with stability region shown in Figure 3.5, appears to be better prepared for such a task.

Now, let us also consider the full-drift implicit Euler scheme

$$Y_{n+1} = Y_n + a(Y_{n+1})\Delta + b(Y_n)\Delta W_n$$

with transfer function

$$G_{n+1}(\lambda\,\Delta, \alpha) = \left| \frac{1 + \sqrt{-\alpha\,\lambda}\,\Delta W_n}{1 - \left(1 - \frac{3}{2}\,\alpha\right)\lambda\,\Delta} \right|.$$

Figure 4.2 shows its stability region which looks similar to the region obtained for the semi-drift implicit Euler scheme. However, it has an additional area of stability for α close to 1 and $\lambda\Delta$ near -10. Additionally, this region diminishes as p becomes larger and does not cover the martingale case $\alpha = 2/3$. It appears

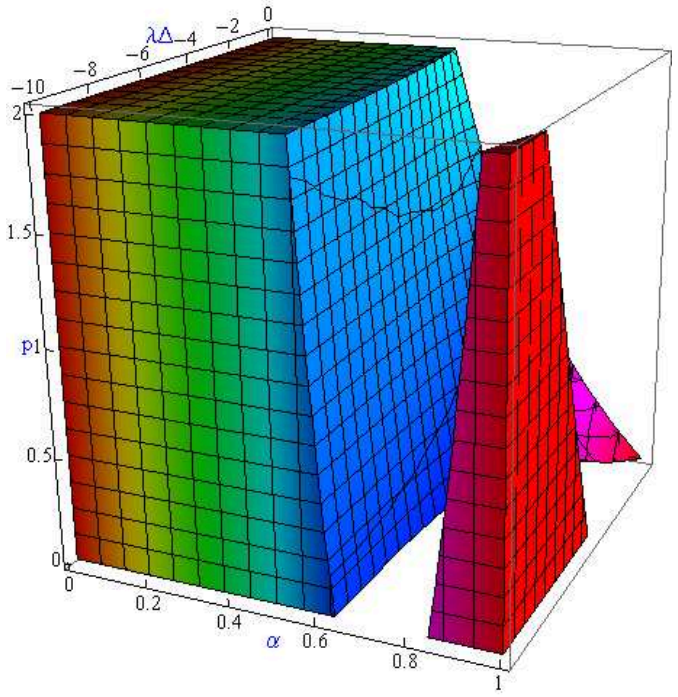

Figure 4.2: Stability region for full-drift implicit Euler method.

that the region of stability is likely to increase with the degree of implicitness in the drift term of an implicit Euler scheme. However, this increase of asymptotic p-stability seems to weaken as p becomes large.

Finally, we mention in this section the balanced implicit Euler method, proposed in Milstein, Platen & Schurz (1998). We study this scheme in the particular form

$$Y_{n+1} = Y_n + \left(1 - \frac{3}{2}\,\alpha\right) \lambda Y_n \Delta + \sqrt{\alpha|\lambda|} Y_n \Delta W_n + c|\Delta W_n|(Y_n - Y_{n+1}).$$

When c is chosen to be $\sqrt{-\alpha\,\lambda}$, then its transfer function equals

$$G_{n+1}(\lambda\,\Delta, \alpha) = \left| \frac{1 + \left(1 - \frac{3}{2}\,\alpha\right) \lambda\,\Delta + \sqrt{-\alpha\,\lambda}\,(\Delta W_n + |\Delta W_n|)}{1 + \sqrt{-\alpha\,\lambda}|\Delta W_n|} \right|.$$

The corresponding stability region is shown in Figure 4.3.

It turns out that this is the only type of method we have considered so far that provides in the martingale case $\alpha = 2/3$ for small values of p, asymptotic p-stability for all $\lambda\Delta$, this means, also for large step sizes. Consequently, the balanced implicit Euler method is well suited for the scenario simulation of martingales for which it was originally designed, see Milstein, Platen & Schurz (1998). Note that one has flexibility in designing a range of balanced implicit methods.

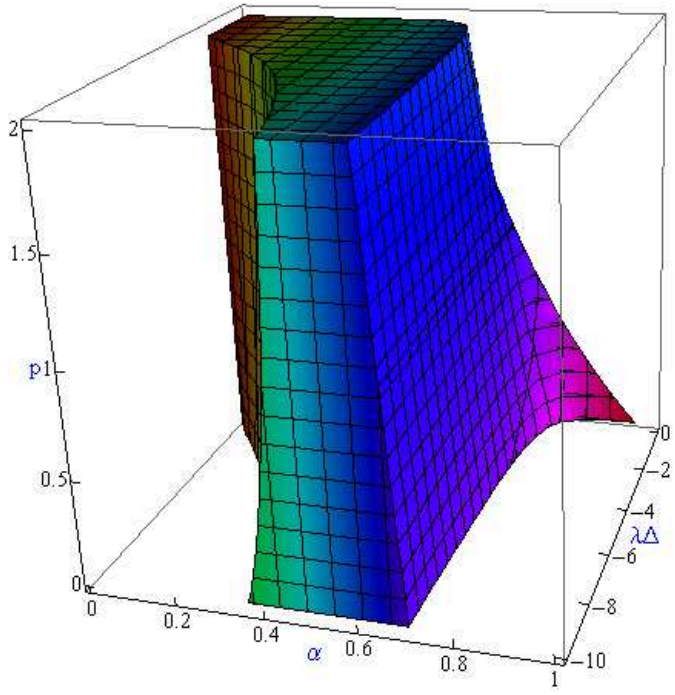

Figure 4.3: Stability region for a balanced implicit Euler method.

5 Stability of Simplified Methods

All the schemes considered so far were originally designed for scenario simulation, see Kloeden & Platen (1999). However, Monte Carlo simulation is extremely important in finance and requires only weak approximations. The Wiener process increments ΔW_n, appearing in a Taylor scheme, can be typically replaced in a weak scheme by simpler multi-point random variables, see Kloeden & Platen (1999). These need to satisfy certain moment matching conditions for a given weak order of convergence. In most of the previous schemes the Gaussian random variable ΔW_n may be replaced by a simpler two point distributed random variable $\Delta \hat{W}_n$, which has probabilities

$$P(\Delta \hat{W}_n = \pm\sqrt{\Delta}) = \frac{1}{2}. \tag{5.1}$$

Numerical schemes using random variables of the type $\Delta \hat{W}_n$ are called "*simplified*". They can be employed in Monte Carlo simulation but are not suited for scenario simulation, see Kloeden & Platen (1999).

We have investigated the impact of such simplified random variables in weak schemes on the corresponding stability regions. The resulting stability regions look, in some sense, similar to those of the corresponding previously studied schemes. In most cases, the stability region increases slightly. To provide an example, Figure 5.1 shows the stability region of the simplified symmetric predictor-

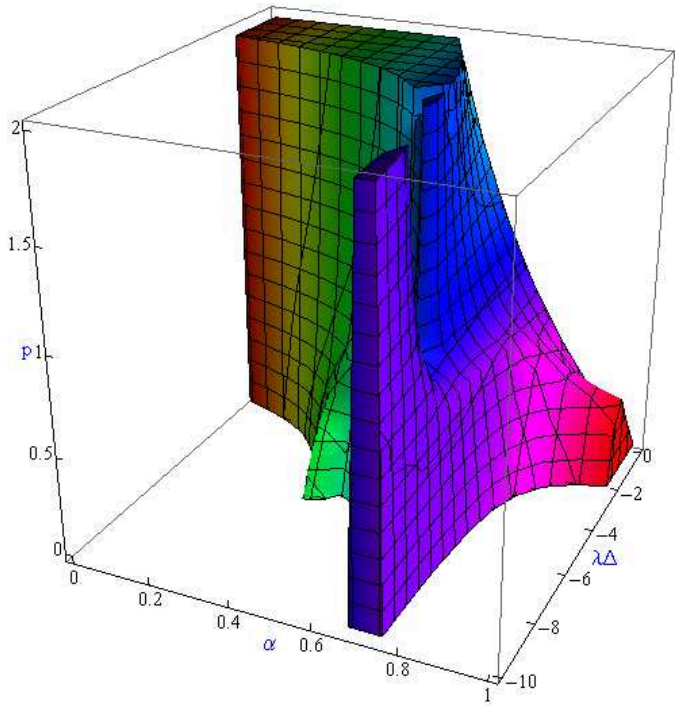

Figure 5.1: Stability region for the simplified symmetric predictor-corrector Euler method.

corrector Euler scheme. It is, of course, different from the one shown in Figure 3.5 but has certain similarities. When comparing these two figures, the simplified scheme presents an increased stability region, in particular near the level $\alpha \approx 2/3$, which is critical for the Monte Carlo simulation of martingales. In general, one can say that simplified schemes increase numerical stability. The stability region of the simplified balanced implicit Euler method is similar to the one already presented in Figure 4.3 and is, therefore, not displayed.

As pointed out in Kloeden & Platen (1999), in a simplified weak scheme, terms that approximate the diffusion coefficient can also be made implicit. The reason being that in a simplified scheme, instead of using an unbounded Gaussian random variable ΔW_n, one uses a bounded random variable $\Delta \hat{W}_n$. Let us now consider the family of simplified implicit Euler schemes, see Kloeden & Platen (1999), given in the form

$$\begin{aligned} Y_{n+1} &= Y_n + \{\theta\, \bar{a}_\eta(Y_{n+1}) + (1-\theta)\bar{a}_\eta(Y_n)\}\, \Delta \\ &\quad + \{\eta\, b(Y_{n+1}) + (1-\eta)\, b(Y_n)\}\, \Delta \hat{W}_n, \end{aligned} \tag{5.2}$$

for $\theta, \eta \in [0,1]$ and $\bar{a}_\eta = a - \eta b b'$. When comparing this scheme with the strong predictor-corrector Euler scheme (3.3), one notices a resemblance to its corrector part. For sufficiently small step size Δ, the implicitness in the diffusion term

makes sense for this scheme. Its transfer function is of the form

$$G_{n+1}(\lambda\,\Delta,\alpha) = \frac{1+(1+(\eta-\frac{3}{2})\alpha)\lambda(1-\theta)\Delta+(1-\eta)\sqrt{\alpha|\lambda|}\Delta\hat{W}_n}{1-(1+(\eta-\frac{3}{2})\alpha)\lambda\theta\Delta-\eta\sqrt{\alpha|\lambda|}\Delta\hat{W}_n}. \tag{5.3}$$

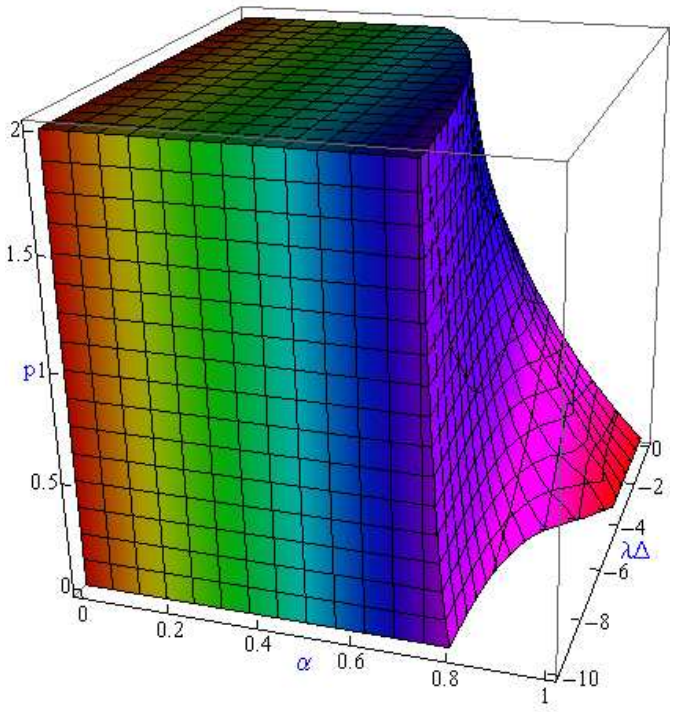

Figure 5.2: Stability region for the simplified symmetric implicit Euler Scheme.

We have studied the resulting stability regions for this family of schemes. For instance, the stability region for the simplified semi-drift implicit Euler scheme resembles that in Figure 4.1, and that of the simplified full-drift implicit Euler method shown in Figure 4.2. The stability region of the simplified symmetric implicit Euler scheme with $\theta = \eta = 0.5$ in (5.2) is presented in Figure 5.2, and that of the simplified fully implicit Euler method is shown in Figure 5.3. We observe that both stability regions fill almost the entire area covered. This indicates that a simplified symmetric or fully implicit Euler scheme could overcome potential numerical instabilities in Monte Carlo simulation. Note that we achieve here asymptotic p-stability even in some situations where the test dynamics are not asymptotically p-stable.

However, we point out that for the simplified symmetric implicit Euler scheme, see Figure 5.2, problems may arise for small step sizes. For instance, for the martingale case, that is $\alpha = 2/3$, a problem occurs at $p = 2$, the stability region is decreased by the use of a time step size that is too small. This means, for an implementation which may have been successfully working for some given time using a large step size in a derivative pricing tool, by decreasing the time step

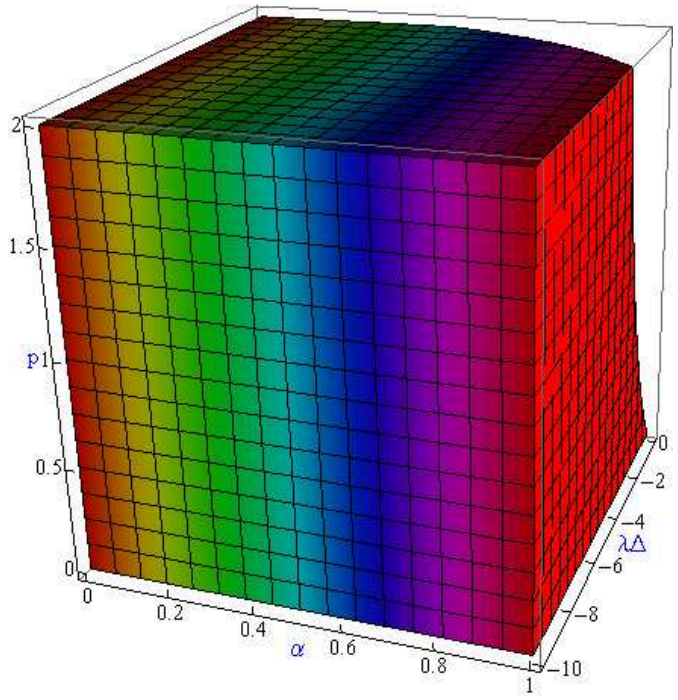

Figure 5.3: Stability region for the simplified fully implicit Euler Scheme.

size, often expecting a more accurate valuation, one can in fact create severe numerical stability problems. This type of effect has already been observed in Section 3 for several predictor-corrector Euler methods. We observe this interesting phenomenon here even for a fully implicit scheme. Refining the time step size in a simulation can, therefore, lead to numerical stability problems where errors are uncontrollably propagated.

Finally, we perform some Monte Carlo simulations, where we estimate the first absolute moment of X_T for $T \in [0, 20]$, $\lambda = -3/2$, $\alpha = 2/3$ and $\Delta = 2$. We simulate 100,000 sample paths to obtain extremely small confidence intervals, which we subsequently neglect in Figure 5.4, where we show the absolute error between the absolute first moment of the test dynamics calculated using the exact solution X_T and the simplified symmetric predictor-corrector Euler scheme Y_T for $T \in [0, 20]$.

One can observe that the Monte Carlo simulation with the simplified symmetric predictor-corrector Euler scheme performs much better than the simplified Euler scheme when compared to Figure 1.2. The better performance is explained by the fact that this scheme stays for $p = 1$ in its stability region, whereas the simplified Euler scheme, is for the given parameters, in a region where there is no asymptotic p-stability when p equals one.

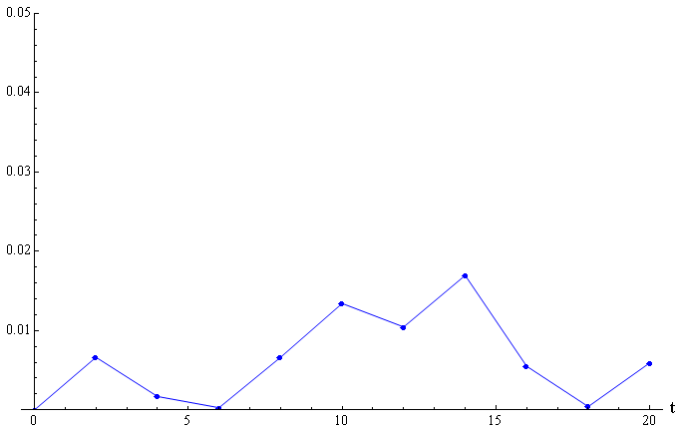

Figure 5.4: Absolute error of the simulated absolute first moment for the simplified symmetric predictor-corrector Euler scheme.

Conclusion

We have presented an approach to the study of asymptotic p-stability of discrete time approximate solutions of stochastic differential equations with emphasis on martingales, which are relevant in finance when simulating asset prices. It has been demonstrated that implicit methods provide the largest stability regions, whereas the standard Euler scheme and other explicit methods have rather restricted stability regions. The symmetric predictor-corrector Euler scheme exhibits reasonable numerical stability properties. The stability analysis of a range of schemes revealed that by refining the time step size a scheme can become numerically unstable. Consequently, the common view formed in deterministic numerical analysis that by reducing the time step size one always retains numerical stability may have to be modified in a stochastic setting.

Acknowledgment

The authors express their deep sadness about the tragic death of their dear colleague Nicola Bruti-Liberati on his way to work on 28 August 2007. He inspired some of the work presented in this paper. The valuable suggestions of two referees improved significantly the final version of the paper.

References

Alcock, J. T. & K. Burrage (2006). A note on the balanced method. *BIT Numerical Mathematics* **46**, 689–710.

Bruti-Liberati, N. & E. Platen (2008). Strong predictor-corrector Euler methods for stochastic differential equations. *Stochastics and Dynamics* **8**(3),

561–581.

Glasserman, P. (2004). *Monte Carlo Methods in Financial Engineering*, Volume 53 of *Appl. Math.* Springer.

Hairer, E. & G. Wanner (1996). *Solving Ordinary Differential Equations II, Stiff and Differential Algebraic Systems* (2nd ed.). Springer.

Hasminski, R. Z. (1980). *Stochastic Stability of Differential Equations*. Sijthoff & Noordhoff, Alphen naan den Rijn.

Hernandez, D. B. & R. Spigler (1992). *A*-stability of implicit Runge-Kutta methods for systems with additive noise. *BIT* **32**, 620–633.

Hernandez, D. B. & R. Spigler (1993). Convergence and stability of implicit Runge-Kutta methods for systems with multiplicative noise. *BIT* **33**, 654–669.

Higham, D. (2004). *An Introduction to Financial Option Valuation: Mathematics, Stochastics and Computation*. Cambridge University Press.

Higham, D. & P. Kloeden (2005). Numerical methods for nonlinear stochastic differential equations with jumps. *Numer. Math.* **110**(1), 101–119.

Higham, D. J. (2000). Mean-square and asymptotic stability of numerical methods for stochastic ordinary differential equations. *SIAM J. Numer. Anal.* **38**, 753–769.

Higham, D. J., X. Mao, & C. Yuan (2007). Almost sure and moment exponential stability in the numerical simulation of stochastic differential equations. *SIAM J. Numer. Anal.* **45**, 592–609.

Hofmann, N. & E. Platen (1994). Stability of weak numerical schemes for stochastic differential equations. *Comput. Math. Appl.* **28**(10-12), 45–57.

Hofmann, N. & E. Platen (1996). Stability of superimplicit numerical methods for stochastic differential equations. *Fields Inst. Commun.* **9**, 93–104.

Jäckel, P. (2002). *Monte Carlo Methods in Finance*. Wiley.

Klauder, J. R. & W. P. Petersen (1985). Numerical integration of multiplicative-noise stochastic differential equations. *SIAM J. Numer. Anal.* **6**, 1153–1166.

Kloeden, P. E. & E. Platen (1992). Higher order implicit strong numerical schemes for stochastic differential equations. *J. Statist. Phys.* **66**(1/2), 283–314.

Kloeden, P. E. & E. Platen (1999). *Numerical Solution of Stochastic Differential Equations*, Volume 23 of *Appl. Math.* Springer. Third printing, (first edition (1992)).

Kloeden, P. E., E. Platen, & H. Schurz (2003). *Numerical Solution of SDEs Through Computer Experiments*. Universitext. Springer. Third corrected printing, (first edition (1994)).

Milstein, G. N. (1988). A theorem of the order of convergence of mean square approximations of systems of stochastic differential equations. *Theory Probab. Appl.* **32**, 738–741.

Milstein, G. N. (1995). *Numerical Integration of Stochastic Differential Equations*. Mathematics and Its Applications. Kluwer.

Milstein, G. N., E. Platen, & H. Schurz (1998). Balanced implicit methods for stiff stochastic systems. *SIAM J. Numer. Anal.* **35**(3), 1010–1019.

Platen, E. (1995). On weak implicit and predictor-corrector methods. *Math. Comput. Simulation* **38**, 69–76.

Platen, E. & D. Heath (2006). *A Benchmark Approach to Quantitative Finance*. Springer Finance. Springer.

Protter, P. (2005). *Stochastic Integration and Differential Equations* (2nd ed.). Springer.

Saito, Y. & T. Mitsui (1993a). Simulation of stochastic differential equations. *Ann. Inst. Statist. Math.* **45**, 419–432.

Saito, Y. & T. Mitsui (1993b). T-stability of numerical schemes for stochastic differential equations. *World Sci. Ser. Appl. Anal.* **2**, 333–344.

Saito, Y. & T. Mitsui (1996). Stability analysis of numerical schemes for stochastic differential equations. *SIAM J. Numer. Anal.* **33**(6), 2254–2267.

Talay, D. (1982). Convergence for each trajectory of an approximation scheme of SDE. *Computes Rendus Acad. Sc. Paris, Séries I Math.* **295**(3), 249–252. (in French).